PRODUCTION OF CARBON NANOTUBES AND HYDROGEN BY CATALYTIC ETHANOL DECOMPOSITION

PRODUCCIÓN DE NANOTUBOS E HIDRÓGENO MEDIANTE LA DESCOMPOSICIÓN CATALÍTICA DE ETANOL

JAIME GALLEGO

Ph.D. Instituto de Química, Universidad de Antioquia, Medellín-Colombia, jaimegallegomarin@yahoo.es

GERMÁN SIERRA GALLEGO

Ph.D. Escuela de Ingeniería de Materiales, Facultad de Minas, Universidad Nacional de Colombia, Medellín-Colombia, geasierraga@unal.edu.co

CARLOS DAZA

Ph.D. Pontificia Universidad Javeriana, Departamento de Química, Bogotá, Colombia, carlosenriquedaza@hotmail.com

RAFAEL MOLINA

Ph.D. Departamento de Química, Universidad Nacional de Colombia, Bogotá-Colombia. ramolinag@unal.edu.co

JOËL BARRAULT

Ph.D. IC2MP,UMR CNRS 7285, ENSIP, Université de Poitiers, 1 rue Marcel Doré, 86022. Poitiers-France. joel.barrault@univ-poitiers.fr

CATHERINE BATIOT-DUPEYAT

Ph.D. IC2MP,UMR CNRS 7285, ENSIP, Université de Poitiers, 1 rue Marcel Doré, 86022. Poitiers-France catherine.batiot.dupeyrat@univ-poitiers.fr

FANOR MONDRAGÓN

Ph.D. Instituto de Química, Universidad de Antioquia, Medellín-Colombia, fmondra@gmail.com

Received for review April 17 th, 2012, accepted September 27th, 2012, final version October, 10 th, 2012

ABSTRACT: This work reports the synthesis of multiwall carbon nanotubes (MWCNTs) by the catalytic decomposition of ethanol using the perovskite-type oxide $LaNiO_3$ as catalyst precursor. The carbon nanotubes were characterized by transmission electronic microscopy (TEM), scanning electronic microscopy (SEM) and thermogravimetric analysis (TGA). TEM micrographs show that the carbon nanotubes were multi-walled with inner diameters ranging from 3 nm to 12 nm and outer diameters up to 42 nm. The yield of CNT and H_2 were 3.5 $g_{CNT}\cdot(g_{cat}\cdot h)^{-1}$ and 39 $L_{H2}\cdot(g\cdot h)^{-1}$ respectively at 700 °C. TGA data show that nanotube carbon purity was about 95 % by weight and the oxidation temperature was around 620 °C.

KEY WORDS: Carbon nanotubes, perovskites, nickel, hydrogen, ethanol decomposition.

RESUMEN: En este trabajo se sintetizaron nanotubos de carbono multicapa (MWCNTs) por medio de la reacción de descomposición de etanol usando como precursor del catalizador a la perovskita $LaNiO_3$. Los nanotubos de carbono de pared múltiple (MWCNTs) fueron caracterizados por microscopía electrónica de transmisión (TEM) y de barrido (SEM) y análisis termogravimétrico (TGA). Mediante SEM se observó que los MWCNTs poseen diámetros internos entre 3 nm y 12 nm con diámetros externos de hasta 42 nm, igualmente se observaron algunas partículas metálicas encapsuladas dentro de los nanotubos. La producción de CNT e H_2 fue de 3,5 $g_{CNT}\cdot(g_{cat}\cdot h)^{-1}$ y 39 $L_{H2}\cdot(g\cdot h)^{-1}$ respectivamente a 700 °C. Por TGA se encontró que la pureza de los nanotubos es alrededor del 95 % en peso y su temperatura de oxidación alrededor de 620 °C.

PALABRAS CLAVE: Nanotubos de carbono, Perovskitas, Níquel, Hidrógeno, descomposición de etanol.

1. INTRODUCTION

Carbon nanotubes are an allotropic form of carbon as is graphite, diamond and fullerenes. These materials present many interesting electrical, mechanical, electro-optical and chemical properties. Carbon nanotubes are the ideal material for many applications [1].

Carbon nanotubes can be synthetized by different methods like laser ablation, electric-arc, chemical vapor deposition (CVD), among others [2]. CVD synthesis appears to be a promising technique due to its high performance and easy application. There are many types of catalysts that can be used for CVD synthesis. The most common catalysts are based on transition

metals such as Fe, CO and Ni, and the most used carbon sources are methane, carbon monoxide, hydrocarbons and alcohols such as methanol and ethanol[3].

Carbon nanotubes produced from biogas, bioethanol and biodiesel, can be an alternative option to carbon sequestration with the advantage that recoverable products like carbon nanotubes and hydrogen can be obtained by this methodology.

Production of carbon nanotubes from ethanol decomposition is a carbon capture system because that converts the carbon atoms in the ethanol molecule into a solid form. In this way, carbon is removed from the natural carbon cycle.

Carbon nanotube formation by catalytic methods depends on the size of the metallic particles of the catalysts. Govindaraj et al. [3] reported that with metallic particles as small as 5 nm it is possible to obtain single wall carbon nanotubes (SWCNTs), with metallic particles between 10 nm and 50 nm, it is possible to obtain multiwall carbon nanotubes (MWCNTs) and with metallic particles with diameters larger than 50 nm it is not possible to obtain carbon nanotubes. Large size metallic particles produce "onion" structures where the growth of carbonaceous materials around the metallic particles cause the inhibition of these particles as a place for the growth of carbon nanotubes [3]. However, there are other reports where catalysts with metal particles larger than 50 nm are used to obtain CNTs [4]. In all of these reports it is clear that the size of the metal particles is important for the CNTs growth and for their final properties.

The reduction of some mixed solid oxides such as NiO-MgO, spinels and perovskites, allows the production of a good metallic phase dispersion with a very small particle size [5-7]. As indicated before, low particle size is favorable for the production of CNTs.

In this work, the use of the $LaNiO_3$ perovskite is evaluated as catalyst precursor for ethanol decomposition at atmospheric pressure. The purpose of this reaction is to capture the carbon present in ethanol as carbon nanotubes and at the same time to produce hydrogen. Carbon nanotubes were purified with different methods and characterized with different analytical technics.

2. EXPERIMENTAL METHOD

2.1. Catalyst preparation

The perovskite type oxide $LaNiO_3$ was prepared by the self-combustion method [8]. Glycine ($H_2NCH_2CO_2H$), used as ignition promoter, was added to an aqueous solution of metal nitrates with the appropriate stoichiometry in order to get a NO_3^-/NH_2 = 1 ratio. The resulting solution was slowly evaporated until a vitreous green gel was obtained. The gel was heated up to around 250 °C, temperature at which the ignition reaction occurs producing a powdered precursor which still contains carbon residues. Calcination at 700 °C for 8 h eliminates all of the remaining carbon and leads to the formation of the perovskite structure.

2.2. Ethanol decomposition reaction

Figure 1 shows the schematic diagram of the reaction system used in the decomposition experiments. The reaction was carried out in a horizontal reactor (22 mm internal diameter) in order to avoid pressure variations during the CNT formation. About 50 mg of the catalyst was placed in the reactor and pre-reduced with pure hydrogen (30 $mL \cdot min^{-1}$) at 700 °C for 1 h. The reduced form of the perovskite was Ni/La_2O_3 which is the catalyst for the ethanol decomposition. After purging the catalyst with He, about 0.04 $mL \cdot min^{-1}$ of absolute ethanol was fed to an evaporator using an HPLC pump. Ethanol was evaporated at 120 °C before it came in contact with the catalyst. The ethanol vapor was transported into the reactor using He as a carrier gas at different concentrations (2.6 %, 5 % and 50 % of ethanol in He) and at different total flows (10 $mL \times min^{-1}$, 25 $mL \times min^{-1}$ and 50 $mL \times min^{-1}$). The decomposition reactions were performed at 700 °C.

The gaseous reaction products were analyzed by an on-line mass spectrometer.

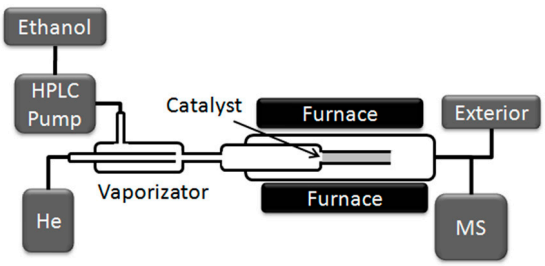

Figure 1. Diagram of experimental apparatus for ethanol decomposition.

Product selectivity S_A was defined as follows:

$$S_A(\%) = \frac{nA_{Det}}{n_{Total,\,Det}} \times 100$$

Where nA_{Det} means detected moles of product A and $n_{Total,Det}$ means total detected moles.

The carbon yield was calculated according to the following equation:

$$CNT_{yield} = \frac{W_{CNTs}}{W_{cat} \cdot t_{rxn}}$$

Where W_{CNTs} is the weight of the carbon deposits, W_{cat} is the catalyst weight and t_{rxn} is the reaction time.

2.3. Purification treatment of carbon nanotubes

The obtained carbonaceous materials were purified by an oxidative methodology. First, an acid treatment was carried out in order to eliminate inorganic components. CNT were treated with 65 % HNO_3. A sample of 100 mg of CNT was dispersed in 50 mL of acid. The mixture was magnetically stirred for 1 h at 25 °C. The product was filtered using a 0.45 µm pore diameter cellulose-ester filter, then washed with deionized water until a neutral pH was obtained. The residue was dried at 100 °C for 24 h, and the CNT weight was determined. The CNT sample obtained as a result was treated with a hydrogen-peroxide solution (10 %) in order to eliminate the amorphous carbon material.

2.4. Thermogravimetric analysis

Thermogravimetric analysis (TGA) of CNTs was carried out in a TA Instruments 2950. Samples were placed in a platinum pan in quantities of 5 mg to 8 mg and heated at 15 °C×min^{-1}, using a high resolution method with resolution 6 and sensitivity 4 [9], from room temperature up to 900 °C under 60 mL×min^{-1} of air.

Scanning Electron Microscopy was carried out using a JEOL JSM 840. The sample was deposited on a graphite tape and coated with a nano-film of cadmium-gold.

High-resolution transmission electron microscopy (HR-TEM) was carried out using a JEOL 2100UHR instrument with a LaB_6 filament, at a 200kV accelerating voltage. HR-TEM images of deposited carbon were taken after acid treatment of the sample. The sample was crushed and dispersed in isopropanol. A drop of this solution was deposited on a Cu grid for TEM observations.

3. RESULTS

3.1. Catalyst characterization

Previous papers have reported that the self-combustion method leads to the formation of $LaNiO_3$ perovskite structure after calcination at 700 °C in air [6, 10-12].

In-situ XRD and TPR measurement indicates that after the reduction treatment under hydrogen at 700 °C, $LaNiO_3$ perovskite structure was completely destroyed, the only phases detected being Ni° and La_2O_3. Complete reduction of $LaNiO_3$ takes place around 600 °C [12, 13].

Analysis of the TEM micrographs of the reduced $LaNiO_3$ show that the nickel particles have a size distribution between 2 nm and 50 nm. The average particle size is around 15 nm [10]. This result suggests that the rare earth oxide La_2O_3, can prevent agglomerations of the transition metal and promotes the dispersion of Ni particles at nano-scale, which has been reported as a very advantageous condition for CNT growth [14].

3.2. Ethanol decomposition reaction

The results of ethanol conversion and products selectivity at different temperatures using Ni°/La_2O_3 catalyst are presented in Figure 2. Ethanol catalytic decomposition at 400 °C is very high, near to 100 % conversion. This temperature is much lower than the one required for thermal ethanol activation (700 °C). In the same figure it is also shown that hydrogen production is a maximum when the reaction was performed between 600 °C and 700 °C, with selectivities of 78 % y 81 % respectively.

The effect on the conversion, hydrogen selectivity and carbon nanotubes production was studied at different ethanol concentrations and total flow of reactants.

Figures 3 and 4 display the results of product selectivities at different ethanol compositions (2 %, 5

% and 6 %) at constant flow rates. Figures 4 and 5 show the effect of changing flow rates (10 mL·min^{-1} and 50 mL·min^{-1}) at constant ethanol concentration.

Figures 3 and 4, show that changes in ethanol concentration modify the selectivities of products. When ethanol concentrations of 2 % and 6 % are used, the production of CO_2 and CO is elevated. This result suggests that catalyst participate in the CO_2 production since the selectivity values are the opposite of those obtained in thermal decomposition. [15].

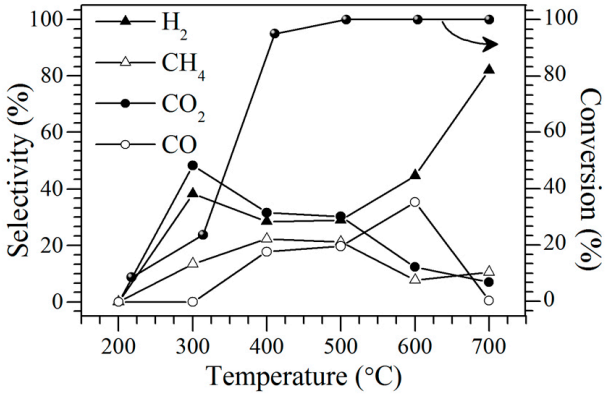

Figure 2. Gases produced in the ethanol conversion and product selectivities at different temperature. Catalyst weight: 50 mg, Gas flow: 25 mL×min^{-1} (2.6 % of ethanol in He).

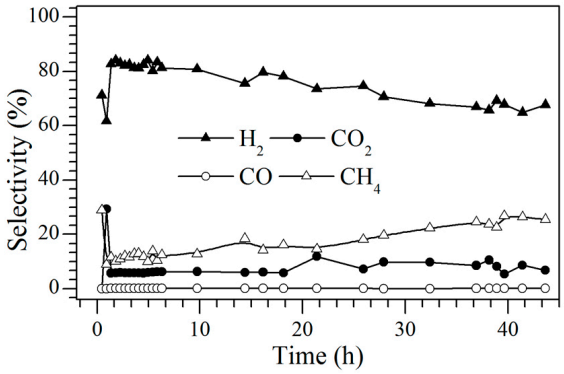

Figure 3. Gas selectivities obtained with 50 mg of catalyst, reaction flow 25 mL×min^{-1} (2 % and 6 % of ethanol in He). Temperature 700 °C.

The catalyst can promote the disproportion reaction of CO (eq. 1).

$$2CO \rightarrow C + CO_2 \qquad (eq.1)$$

Methane selectivity does not vary with changes in the percentage of ethanol, but the hydrogen selectivity decreases with increasing ethanol concentration. This observation indicates that hydrogen can be used to form other products such as hydrocarbons or oxygenated organic compounds which were evidenced by mass spectrometry but were impossible to be quantified due to the low concentrations. Among the compounds identified were acetaldehyde, formaldehyde, ethane and ethylene.

When a reaction flux of 50 mL×min^{-1} was used, no important differences of the selectivities were observed. For the reaction performed at 10 mL·min^{-1}, Figure 4 shows that the initial selectivity of methane is 10 % but that a deactivation during the reaction was observed, increasing the methane selectivity to 20 %.

As shown in Figures 5 and 6 there is a tendency to increase the selectivity to hydrogen when the methane selectivity is lower. This behavior suggests that in the reaction mechanism, much of carbonaceous deposits (CNTs) are produced according to the reaction of cracking of methane (Eq. 2)

$$CH4 \rightarrow C(H)x + \left(2 - x/2\right)H_2 \qquad (eq.2)$$

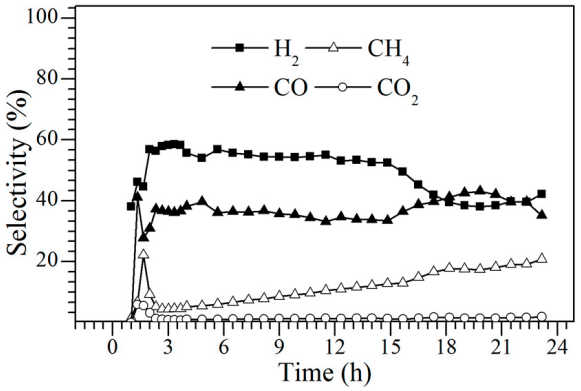

Figure 4. Gas selectivities were obtained with 50 mg of catalyst, reaction flow rate 25 mL×min^{-1} (5 % of ethanol in He).

Table 1 shows that the production of hydrogen and carbon material for each one of the above conditions is proportional to the amount of ethanol introduced. This behavior suggests that the reaction can be used as a process for carbon sequestration. The results show that the selectivity toward carbon deposition is independent of the flow of ethanol.

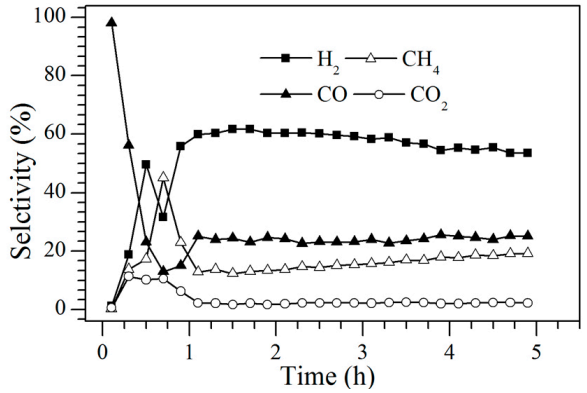

Figure 5. Gas selectivities obtained with 50 mg of catalyst, reaction flow rate 10 mL×min^{-1} (50 % of ethanol in He).

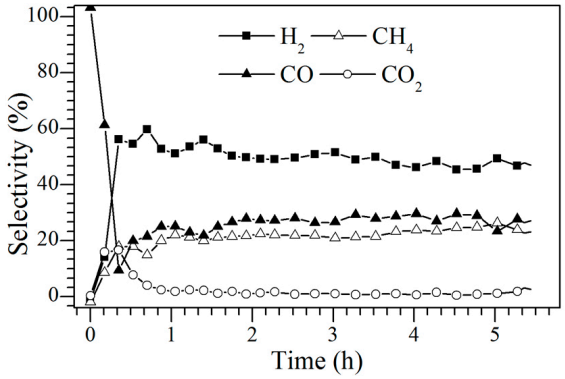

Figure 6. Gas selectivities obtained with 50 mg of catalyst, reaction flow rate 50 mL×min^{-1} (50 % of ethanol in He).

Table 1. Hydrogen and carbon materials production from ethanol thermo-catalytic decomposition.

Reaction conditions			Carbon deposits		Hydrogen flow rate	
	Ethanol				A	B
Total flow rate (mL·min^{-1})	%	mL·min^{-1} (gas)	mg	mg·h^{-1}	L·(h·g$_{cat}$)$^{-1}$	L_{H2}·(L_{EtOH}·g$_{cat}$)$^{-1}$
25	2,6	0,65	357,2	8,1	34,1	874,4
25	5	1,25	456,0	19	36,5	486,7
10	50	5	340,3	85,1	14,8	49,3
50	50	25	819,7	204,8	39,08	26,1

B: values determined by dividing column A by the flow rate of ethanol.

Table 1 shows that selectivity towards hydrogen decreases with increasing the ethanol flow, while the amount of carbon deposits increases, suggesting that the mechanisms of cracking of hydrogenated species is affected by the amount of ethanol per unit of time and the amount of the catalyst in the reactor. One possible reason is that carbon deposits inhib7/it the catalytic¿reaction that leads to hydrogen production.

3.3. Characterization of carbon deposits by SEM and TEM.

Figure 7a-c shows the electron micrographs for carbon deposits obtained after the reaction. These SEM micrographs show clear evidence of the formation of filaments, which may be carbon nanotubes or carbon nanofibers. Additionally, there are some small agglomerates which can be attributed to amorphous carbon (Figure 7c).

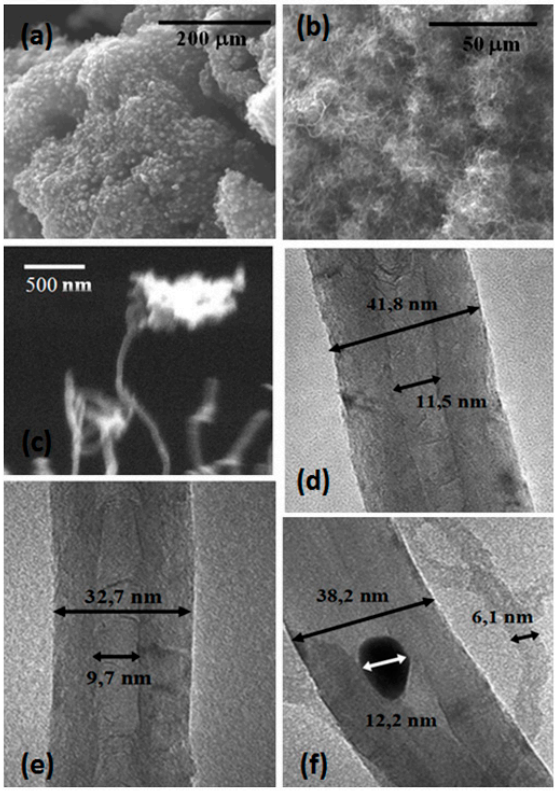

Figure 7. Scanning (a-c) and transmission (d-f) electronic micrographs for the carbon deposits after reaction.

The nature of the carbon deposits was verified using transmission electron microscopy. In Figure 7d-f multi-wall carbon nanotubes with outer diameters ranging from 6 nm to 75 nm and inner diameter from 4

nm to 12 nm can be distinguished. Also encapsulated metal particles inside the carbon nanotubes are observed. This has already been reported and it is probably due to the CNT's growing mechanism [1].

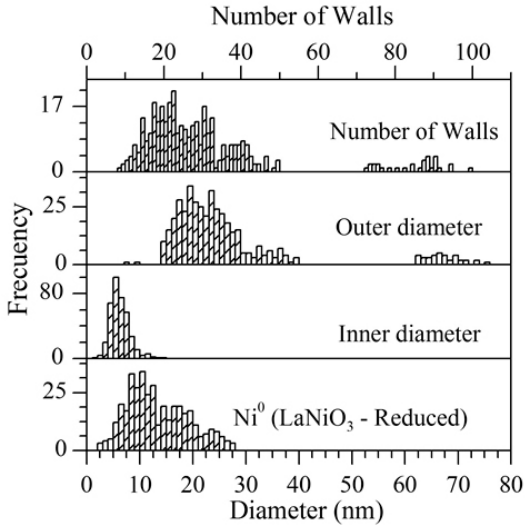

Figure 8. Catalyst metal particle size, inner diameters, outer diameters and wall number distributions of carbon nanotubes.

Figure 8 shows the diameter distribution of carbon nanotubes, nickel particle size distribution and the number of walls of carbon nanotubes determined from TEM micrographs.

The internal diameter of carbon nanotubes is about 25 % lower than the size of the metallic particles, which agrees with the proposed growth mechanisms for these materials [15].

It is also observed that there is no connection between the outer diameter of the carbon nanotubes and the metallic particles size or the inner diameter of the nanotubes. This suggests that the outer diameter is more related to the experimental reaction conditions than to the metallic particle size. In some cases, the catalyst derived from $LaNO_3$ perovskite can generate CNTs with an outer diameter of 75 nm. The average nickel particle size is close to 12 nm while the outer diameter of the carbon nanotubes is much higher. The TEM data indicates that CNT can be formed up to about six times the particle size of Ni. This is a very long range induction effect of the Ni particles which does not have a clear explanation at the moment.

3.4. TGA characterization of carbon nanotubes.

As reported in the literature, carbon nanotubes have a higher oxidation temperature than amorphous carbon [13], which can be evidenced by thermogravimetric analysis. Figure 9 displays the thermograms which show that the increase of the ethanol flow rate increases the production of amorphous carbon. The above affirmation is supported by the thermal events observed at low temperatures (400 °C – 520 °C). The production of this amorphous carbon may be due to a saturation of active sites where carbon nanotubes are formed.

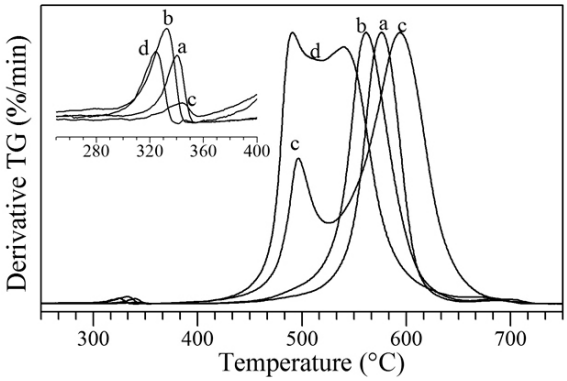

Figure 9. Derivative of the weight loss in thermogravimetric analysis of different CNT's obtained under different ethanol flow rates (a) 2,6 % - 25 mL·min^{-1}, (b) 5 % - 25 mL·min^{-1}, (c) 50 % - 10 mL·min^{-1} y (d) 50 % - 50 mL·min^{-1}.

In a previous investigation [15], it was shown that the carbon nanotube characteristics vary upon changing the carbon precursor, between ethanol and ethanol thermal decomposition products (CH_4, CO, H_2, C_2). The amorphous material content also changes, showing that the different precursors generate different adsorbed species over the catalyst surface. This effect can be observed as well with the change in the ethanol concentrations. At high concentrations of ethanol there will be a saturation of the active sites with carbon atoms, generating other adsorbed species. Those species can be precursors of the amorphous materials. Kura et al. have reported that over nickel particles with a higher diameters (around 100 nm) a polymerization of -CH_3 -CH_2 and –CH species can take place in order to obtain amorphous materials during the hydrogen assisted methane decomposition [16].

In addition, the change in the flow rate of ethanol affected the magnitude of the low-temperature events,

which have been attributed to the oxidation of CH_X species. These CH_X species are presented in both carbon nanotubes and the amorphous material [5].

The purification process of carbon nanotubes was performed on materials with a significant content of amorphous carbon (c). Figures 10 and 11, display the thermograms for the materials after reaction, after purification with nitric acid and after purification with H_2O_2.

The residue found after complete oxidation of carbon species is about 4.0 % wt of the original sample. This residue after oxidation is just NiO, coming from the Ni particles encapsulated inside the carbon nanotubes. It was also noted that the residue (remaining catalyst) only decreases with acid treatment, which is in agreement with the fact the hydrogen peroxide only oxidizes organic materials.

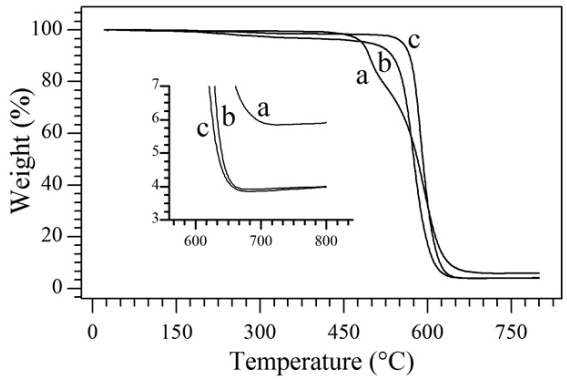

Figure 10. Thermogravimetric analysis of different carbonaceous materials. (a) after reaction, (b) after acid treatment and (c) after peroxide treatment.

Figure 11 shows how after acid treatment the oxidation signal for the amorphous material decreases significantly. This result shows that the acid is capable of oxidizing these structures as reported in the literature [9].

The initial weight loss between 100 °C and 400 °C for purified material, is attributed to the elimination of functional groups such as hydroxyl, carboxyl, nitro and others that can be placed on the nanotubes by acid treatments [17].

The temperature of oxidation of CNTs is around 620 °C and the purity is estimated over 96 %.

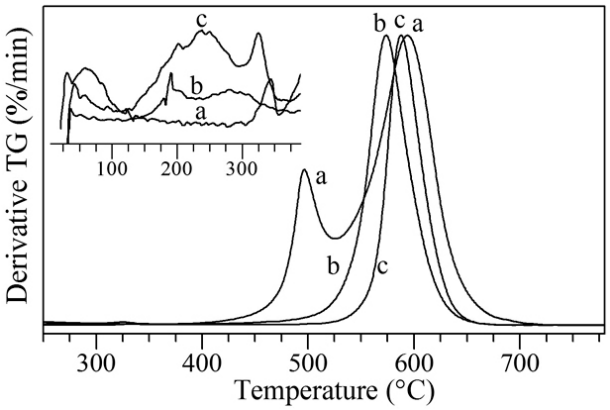

Figure 11. Derivative of thermogravimetric analysis for different carbonaceous materials (a) after reaction, (b) after acid treatment and (c) after peroxide treatment.

4. CONCLUSIONS

This catalyst has a high activity for ethanol decomposition to produce carbon nanotubes and hydrogen. The yields of CNT and H_2 were 3.5 $g_{cnt}\cdot(g_{cat}\cdot h)^{-1}$ and 39 $L_{H2}\cdot(g_{cat}\cdot h)^{-1}$ at 700 °C and 50 $mL\cdot min^{-1}$ of ethanol in He (50 % - v/v).

TEM micrographs show that CNTs were multi-walled, with inner diameters ranging from 3 nm to 12 nm and outer diameter up to about 75 nm and several microns in length.

The inner diameter of carbon nanotubes is proportional to the metallic particle size whereas the outer diameter is related to the experimental reaction conditions.

The CNTs oxidation temperature is around 620 °C which is an indication of the high purity of this material, estimated to be over 96 %.

5. ACKNOWLEDGEMENTS

The authors are grateful to the ECOS-Nord/ Colciencias program for the financial support given. F. Mondragon, J. Gallego and G. Sierra acknowledge the University of Antioquia for the financial support of the "Sostenibilidad" Program 2013-2014. J. Gallego C. Daza and G. Sierra would like to thank Colciencias and the University of Antioquia (JG and GS) for the PhD scholarship.

REFERENCES

[1] De Jong, K. P. and Geus, J. W., Carbon Nanofibers: Catalytic Synthesis and Applications, Cat. Rev. - Sci. Eng., 42, pp. 481-510, 2000.

[2] Harris, P. J. F., Solid state growth mechanisms for carbon nanotubes, Carbon, 45, pp. 229-239, 2007.

[3] Govindaraj, A. and Rao, C. N. R., Synthesis, growth mechanism and processing of carbon nanotubes. En: Carbon Nanotechnology (Eds: Dai L), Elsevier, pp. 15-51, 2006.

[4] Moshkalev, S. A. and Verissimo, C., Nucleation and growth of carbon nanotubes in catalytic chemical vapor deposition, J. Appl. Phys., 102, pp. 4773–4782, 2007.

[5] Djaidja, A., Libs, S., Kiennemann, A. and Barama, A., Characterization and activity in dry reforming of methane on NiMg/Al and Ni/MgO catalysts, Catal. Today, 113, pp. 194-200, 2006.

[6] Sierra, G., Batiot-Dupeyrat, C., Barrault, J., Florez, E. and Mondragón, F., Dry reforming of methane over $LaNi_{1-y}B_yO_{3\pm\delta}$ (B = Mg, Co) perovskites used as catalyst precursor, Appl. Catal.,A: General, 334, pp. 251-258, 2008.

[7] Sierra, G., Batiot-Dupeyrat, C. and Mondragón, F., Methane partial oxidation by the lattice oxygen of the $LaNiO_{3-\delta}$ perovskite. A pulse study, DYNA, 163, pp. 141-150, 2010.

[8] Chick, L. A., Pederson, L. R., Maupin, G. D., Bates, J. L., Thomas, L. E. AND Exarhos, G. J., Glycine-nitrate combustion synthesis of oxide ceramic powders, Mater. Lett., 10, pp. 6-12, 1990.

[9] Musumeci, A. W., Silva, G. G., Martens, W. N., Waclawik, E. R. and Frost, R. L., Thermal decomposition and electron microscopy studies of single-walled carbon nanotubes, J. Therm. Anal. Calorim., 88, pp. 885-891, 2007.

[10] Sierra, G., Batiot-Dupeyrat, C., Barrault, J. and Mondragón, F., Dual Active-Site Mechanism for Dry Methane Reforming over Ni/La_2O_3 Produced from $LaNiO_3$ Perovskite, Ind. Eng. Chem. Res., 47, pp. 9272-9278, 2008.

[11] Sierra, G., Mondragón, F., Barrault, J., Tatibouët, J.-M. and Batiot-Dupeyrat, C., CO_2 reforming of CH_4 over La-Ni based perovskite precursors, Appl. Catal.,A: General, 311, pp. 164-171, 2006.

[12] Sierra, G., Mondragón, F., Tatibouët, J.-M., Barrault, J. and Batiot-Dupeyrat, C., Carbon dioxide reforming of methane over La_2NiO_4 as catalyst precursor--Characterization of carbon deposition, Catal. Today, 133-135, pp. 200-209, 2008.

[13] De Lima, S., Peña, M., Fierro, J. and Assaf, J., $La_{1-x}Ca_xNiO_3$ Perovskite Oxides: Characterization and Catalytic Reactivity in Dry Reforming of Methane, Catal. Lett., 124, pp. 195-203, 2008.

[14] Pan, Z. W., Xie, S. S., Chang, B. H., Sun, L. F., Zhou, W. Y. and Wang, G., Direct growth of aligned open carbon nanotubes by chemical vapor deposition, Chem. Phys. Lett., 299, pp. 97-102, 1999.

[15] Gallego, J., Sierra, G., Mondragon, F., Barrault, J. and Batiot-Dupeyrat, C., Synthesis of MWCNTs and hydrogen from ethanol catalytic decomposition over a Ni/La_2O_3 catalyst produced by the reduction of $LaNiO_3$, Appl. Catal.,A: General, 397, pp. 73-81, 2011.

[16] Kuras, M., Petit, P. and Petit, C., Correlation between the characteristics of multi-wall carbon nanotubes and the structure of the metal oxides used as catalytic precursors for their production, Carbon, 49, pp. 1453-1461, 2011.

[17] Porro, S., Musso, S., Vinante, M., Vanzetti, L., Anderle, M., Trotta, F. and Tagliaferro, A., Purification of carbon nanotubes grown by thermal CVD, Physica E, 37, pp. 58-61, 2007.